Advances in Differential Equations and Control Processes

http://www.pphmj.com
http://dx.doi.org/10.17654/DE023020105
Volume 23, Number 2, 2020, Pages 105-123 **ISSN: 0974-3243**

APPLICATION OF THE DIGITAL RESOLUTION OF ANISOTROPIC AND NONLINEAR DIFFUSION EQUATION TO IMAGE PROCESSING

V. M. Serge Soumanou[1,2], Sounmaïla Moumouni[2], Siaka Massou[1] and Adébayo L. Essoun[1]

[1]Department of Physics
Faculty of Science and Technology
University of Abomey-Calavi
Benin
e-mail: siakmas@yahoo.fr
soumanouserge@yahoo.fr

[2]Higher Teachers Training School of Natitingou
National University of Sciences, Technology, Engineering and Mathematics
Benin
e-mail: sounma.moumouni@gmail.com

Abstract

Techniques based on nonlinear partial differential equations have impacted the image processing field with increasing success supported by experimental results. In this article, we have proposed a 2-dimensional model of image processing by combining anisotropic diffusion with generalized nonlinear diffusion. On the one hand, this model makes it possible to perfectly restore the degraded image with an improvement in the contrast of the image. On the other hand, this

Received: June 8, 2020; Accepted: August 11, 2020
2010 Mathematics Subject Classification: 35K57, 35A24, 35E05, 36B65.
Keywords and phrases: anisotropic diffusion, nonlinear diffusion, segmentation, image restoration.

model allows for the segmentation of images. Various statistical criteria are used to assess the quality of the restored images.

1. Introduction

For several decades nonlinear methods based on partial differential equations (PDE) represent powerful tools in the field of image processing. There are many reasons for this interest: nonlinear effects included in the human visual system (SVH); the highly nonlinear behavior of optical image acquisition systems [1]; obtaining in many cases the results of existence and uniqueness of solution, and even very efficient numerical resolution schemes as in [2, 3]. Although linear filters still play an important role in image processing, being intrinsically very easy to implement, the limitations of this type of filter are well known: images in general do not respect the stationarity hypotheses; linear filters are unable to eliminate noise without blurring the edges. On the other hand, filters from nonlinear approaches can overcome these limitations. The nonlinear diffusion equations which derive from partial differential equations (PDE) are applied in several image processing operations such as restoration [3-12], segmentation [9, 13-22], texture synthesis [23-28]. [29] proposed an unconventional noise filtering algorithm based on differential equations modeling an anisotropic diffusion process. This algorithm served as a reference and stimulated a lot of interest, since it has been widely used by several authors [6, 30-37].

[6] proposed an image processing model by combining the nonlinear and anisotropic diffusion processes. Indeed, the author considered Fisher's nonlinear diffusion equation which not only makes it possible to model the transport mechanisms in living cells [38], but also to enhance the contrast of images [39, 40], which it combined with the anisotropic diffusion equation of [29] in order to obtain a filter which combines the advantages of these two diffusion processes. The model thus proposed by [6] is written in the form:

$$\begin{cases} \dfrac{\partial I(x,\, y,\, t)}{\partial t} = div(g(\| \nabla I(x,\, y,\, t) \|) \cdot \nabla I(x,\, y,\, t)) + f(I(x,\, y,\, t)) \\ t > 0,\ (x,\, y) \in \Omega,\ I(x,\, y,\, 0) = I_0(x,\, y). \end{cases} \quad (1)$$

In this expression, div is the divergence operator, $I(x, y, 0) = I_0(x, y)$ is the original noisy image in a rectangular domain Ω; $I(x, y, t)$ is the image processed at time t; $f(\cdot)$ is a nonlinear cubic function [41, 42] defined by:

$$f(I(x, y, t)) = -\beta I(x, y, t)(I(x, y, t) - \alpha)(I(x, y, t) - 1), \quad (2)$$

where β adjusts the weight of non-linearity and α is the threshold of non-linearity such that $0 < \alpha < 1$; $g(\| \nabla I(x, y, t) \|)$ is a decreasing function proposed by [29] to introduce the anisotropy.

For image processing, the author used an explicit discretization scheme and the results obtained show that this model allows noise filtering and image contrast enhancement while preserving the contours of the image. One of the major shortcomings of this model is its sensitivity to noise. When you increase the noise slightly, you get unsatisfactory results.

The objective of this work is to: modify the model (1) proposed by [6], by combining the anisotropic diffusion of [29] with the generalized model of nonlinear diffusion proposed by [43]; digitally solve this new model for image processing. Thus, we have described in Section 2 the generalized models of nonlinear diffusion and nonlinear anisotropic diffusion. In Section 3, we presented and analyzed the experimental results obtained. Finally, Section 4 presents the conclusion.

2. Proposed Models

2.1. Generalized nonlinear diffusion model

Some homogeneous one-dimensional reaction-diffusion equations have been generalized and solved analytically in [43]. In this work, we propose to write one of these generalized equations in dimension 2 in the following form:

$$\begin{cases} \dfrac{\partial u(x,\, y,\, t)}{\partial t} = \left[\dfrac{\partial^2 u(x,\, y,\, t)}{\partial^2 x} + \dfrac{\partial^2 u(x,\, y,\, t)}{\partial^2 y} \right] \\ \qquad + [1 - u^n(x,\, y,\, t)][au^n(x,\, y,\, t) - \rho]u(x,\, y,\, t), \qquad (3) \\ t > 0,\ (x,\, y) \in \Omega,\ a > 0,\ \rho \neq 0, \text{ and } u(x,\, y,\, 0) = u_0(x,\, y). \end{cases}$$

In this expression, $[1 - u^n(x,\, y,\, t)][au^n(x,\, y,\, t) - \rho]u(x,\, y,\, t)$ is the generalized nonlinear function; a, ρ and n are the parameters of the model. The grid points being with the regular step in the case of the discrete images, to carry out the numerical resolution in order to process the images, [6] used an explicit discretization scheme which we adopted for equation (3) and which gives the following iterative algorithm:

$$u_{i,\,j}^{t+dt} = u_{i,\,j}^{t} + \frac{dt}{|N_r|} \sum_{l,\, m \in N_r} (u_{l,\,m}^{t} - u_{i,\,j}^{t}) + dt(1 - (u_{i,\,j}^{t})^n)(a(u_{i,\,j}^{t})^n - \rho)u_{i,\,j}^{t} \qquad (4)$$

$i,\ j = 1 \ldots N, 1 \ldots M$ are the indices of the pixel of the image to be processed with $N \times M$ the size of the image. $N_r = \{(i-1,\, j);\ (i+1,\, j);\ (i,\, j-1);\ (i,\, j+1)\}$ represents the set of adjacent neighbors of the pixel to be filtered (they are at number of: 4 for the dots in the middle of the image, 3 for the dots on the sides, and 2 for the dots in the corners). $u_{i,\,j}^{t}$ and $u_{i,\,j}^{t+dt}$ are the values of the pixel light intensity at time t and $t + dt$ respectively, dt being the integration step of the differential equation. The image that we want to process is applied to the input of the algorithm and the processed image is recovered at the output.

2.2. Generalized nonlinear anisotropic diffusion model

In this model, we associated the anisotropy of [29] with the generalized nonlinear diffusion process (3), as proposed by [6]. The equation thus obtained is as follows:

$$\begin{cases} \dfrac{\partial u(x,\, y,\, t)}{\partial t} = div(g(\| \nabla u(x,\, y,\, t) \|) \cdot \nabla u(x,\, y,\, t)) \\ \qquad\qquad + [1 - u^n(x,\, y,\, t)][au^n(x,\, y,\, t) - \rho]u(x,\, y,\, t) \\ t > 0,\ (x,\, y) \in \Omega,\ a > 0,\ \rho \neq 0, \text{ and } u(x,\, y,\, 0) = u_0(x,\, y) \end{cases} \quad (5)$$

$g(\| \nabla u(x,\, y,\, t) \|) = \dfrac{1}{1 + \left(\dfrac{\| \nabla u(x,\, y,\, t) \|}{k} \right)^2}$ is the function proposed by [29].

In above, ∇ is the gradient operator; k is a noise estimator [37], or the diffusion barrier which can be defined to preserve the contours of the image. Based on the formula proposed by [37], the value of k calculated by [6] for the image that we want to process is $k = 0.03783$. According to the explicit discretization scheme proposed by [29] for the equation which governs anisotropic diffusion, we deduce the discretized form of equation (5) which is in the form:

$$u_{i,\,j}^{t+dt} = u_{i,\,j}^{t} + \frac{dt}{|\, N_r \,|} \sum_{l,\, m \in N_r} g(\| u_{l,\,m}^{t} - u_{i,\,j}^{t} \|) \times (u_{l,\,m}^{t} - u_{i,\,j}^{t})$$

$$+ dt(1 - (u_{i,\,j}^{t})^n)(a(u_{i,\,j}^{t})^n - \rho)u_{i,\,j}^{t} \quad (6)$$

with $u_{l,\,m}^{t} - u_{i,\,j}^{t}$ an approximation of the local gradient for $(l,\, m) \in N_r$ [29]. Here too, the image that we want to process is applied to the input of the algorithm and the processed image is recovered at the output.

2.3. Evaluation of the quality of restored images

To evaluate the quality of the images restored by the models, we used the criteria of objective evaluation of the approach without reference (*NR*) proposed by [4] since in our study we do not have images of good qualities. According to [4], these objective criteria are defined as follows:

- The mean square error (MSE^O)

$$MSE^o = \frac{1}{M}\frac{1}{N}\sum_{i=1}^{M}\sum_{j=1}^{N}(U^o_{i,j} - U^r_{i,j})^2. \quad (7)$$

- Signal to noise ratio (SNR^o)

$$SNR^o = 10\log\left[\frac{\mu(U^{o2})}{MSE^o}\right]. \quad (8)$$

- The peak signal to noise ratio $(PSNR^o)$

$$PSNR^o = 10\log\left[\frac{\max(U^{o2})}{MSE^o}\right]. \quad (9)$$

In these expressions,

$$\max(U^{o2}) = \max\{(U^o_{i,j})^2\} \text{ and } \mu(U^{o2}) = \frac{1}{M}\frac{1}{N}\sum_{i=1}^{M}\sum_{j=1}^{N}(U^o_{i,j})^2 \quad (10)$$

with U^o the matrix of the degraded image (initial image), and U^r the matrix of the restored image. When the image is well restored (visual appreciation), it has less similarity with the degraded image, so the restored image is good for high values of MSE^o and for low values of SNR^o and $PSNR^o$ [4].

3. Experimental Results and Analysis

3.1. Analysis of restored images

The degraded image of Figure 1 has been restored with the two models proposed in Section 2. Figure 2 presents the results obtained with the generalized model of nonlinear diffusion. This figure shows that there is noise filtering and that the restored image is slightly blurred. This is explained by the isotropic nature of generalized nonlinear diffusion. The evolution of the profile of line 50 of the restored image (Figure 3) shows that the noise is filtered and that there is an increase in the amplitude.

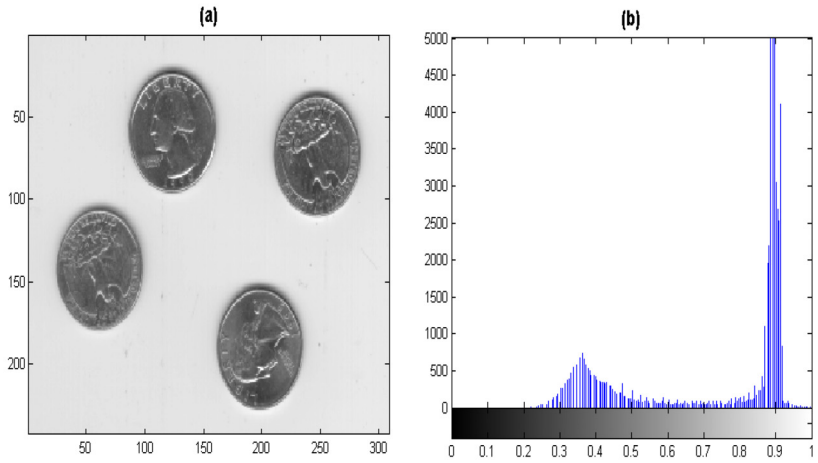

Figure 1. (a) Degraded to restored image and (b) histogram of this image.

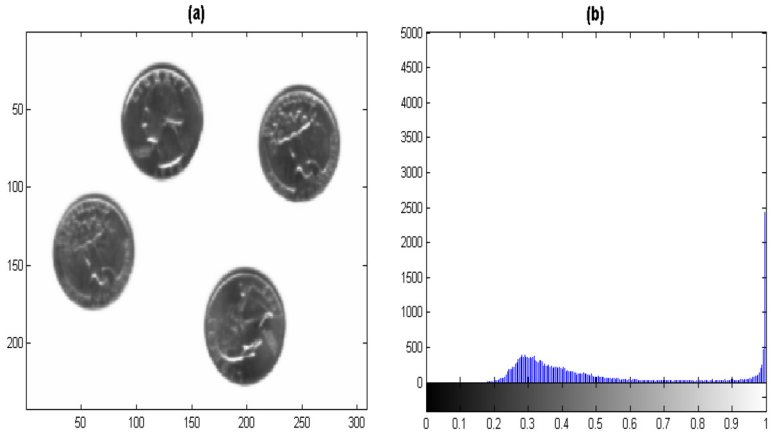

Figure 2. (a) Image restored by our generalized nonlinear diffusion model with the values of the parameters of the model: $a = 1$; $n = 3$; $\rho = 0.1$; $t = 2$; $dt = 0.01$. (b) represents the histogram of this image.

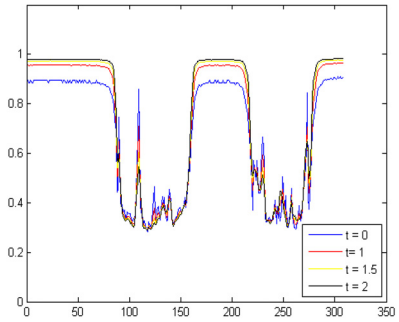

Figure 3. Profile of line 50 of the image restored by our generalized nonlinear diffusion model, for different processing times, with the values of the parameters of the model: $a = 1$; $n = 3$; $\rho = 0.1$; $dt = 0.01$.

With the nonlinear anisotropic diffusion model, the results show that the blurring observed at the level of the image restored with the nonlinear diffusion model disappears and the restored image is sharper (Figure 4). In addition, Figure 5 shows that there is a significant increase in the amplitude of the profile of line 50 of the restored image. This explains a significant increase in contrast and certain details observed on the restored image. In short, the anisotropic diffusion associated with the nonlinear diffusion model promotes very good restoration of the degraded image.

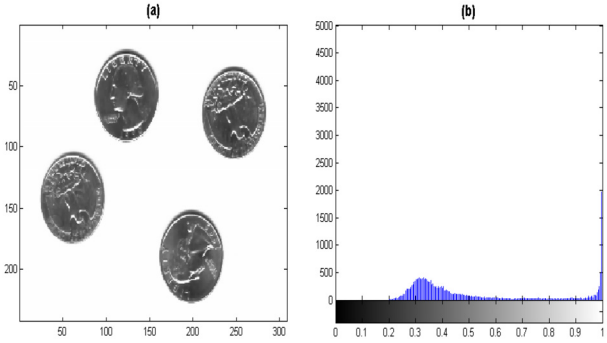

Figure 4. (a) Image restored by our generalized anisotropic and nonlinear diffusion model, with the values of the parameters of the model: $a = 1$; $n = 3$; $\rho = 0.1$; $t = 2$; $dt = 0.01$; $k = 0.03783$. (b) represents its histogram.

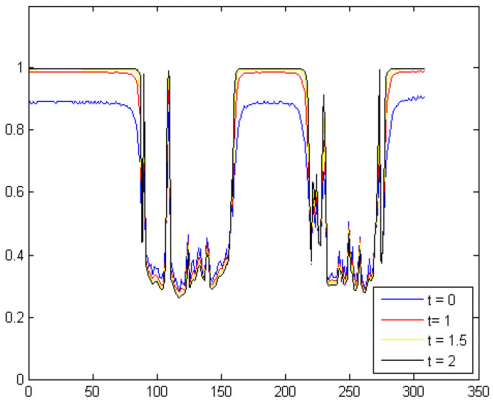

Figure 5. Profile of line 50 of the image restored by our generalized anisotropic and nonlinear diffusion model, for different processing times, with the values of the parameters of the model: $a = 1; n = 3;\ \rho = 0.1; dt = 0.01;\ k = 0.03783$.

Figure 6 (resp. Figure 7) shows the variations of MSE^o, SNR^o and $PSNR^o$ as a function of the processing time of the images, with the generalized model of nonlinear diffusion (resp. with the generalized model of nonlinear anisotropic diffusion). Variations in the three criteria indicate that the quality of the restored images improves as a function of the processing time. The time limit selected, where the restored image is visually of good quality is $t = 2$. This time limit cannot be calculated with these two-dimensional models for which the resolution is digital, unlike the one-dimensional model with analytical solution proposed by [4].

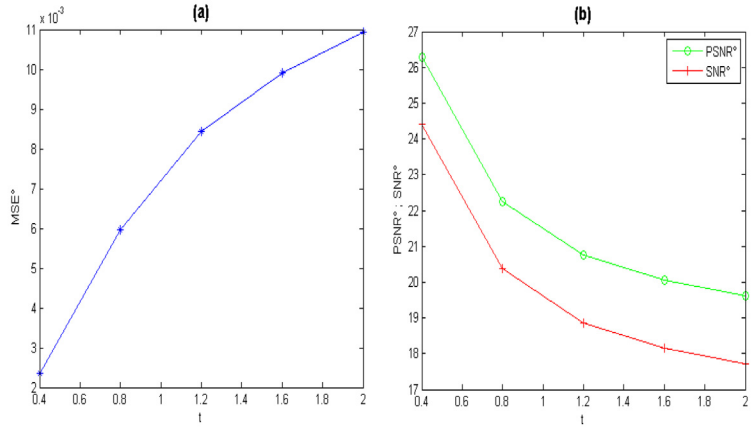

Figure 6. Curves showing the variations of MSE^o, SNR^o and $PSNR^o$ as a function of image processing time, with the generalized nonlinear diffusion model, for the values of the parameters of the model: $a = 1$; $n = 3$; $\rho = 0.1$; $dt = 0.01$.

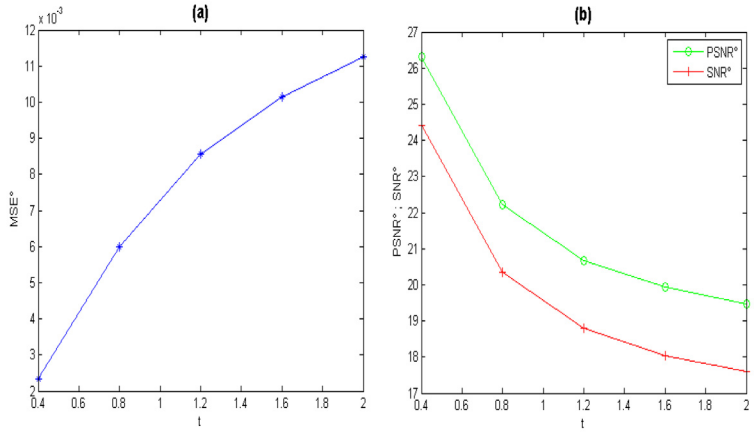

Figure 7. Curves showing the variations of MSE^o, SNR^o and $PSNR^o$ as a function of image processing time, with the generalized anisotropic and nonlinear diffusion model, for the values of the parameters of the model: $a = 1$; $n = 3$; $\rho = 0.1$; $dt = 0.01$; $k = 0.03783$.

With Figure 8, we compare over the same image processing time interval, the values of SNR^o and $PSNR^o$ from our models to those from models proposed by [6]. The results in this figure indicate that the image is better restored, over this time interval, by our models than by the models proposed by [6]. The time limit retained by [6] is $t = 6$ whereas in our case $t = 2$. Figure 9 shows, at $t = 2$, the images restored by the models proposed by [6] and the images restored by our models. We note, for this processing time, that the images restored by our models are better than those restored by the models proposed by [6].

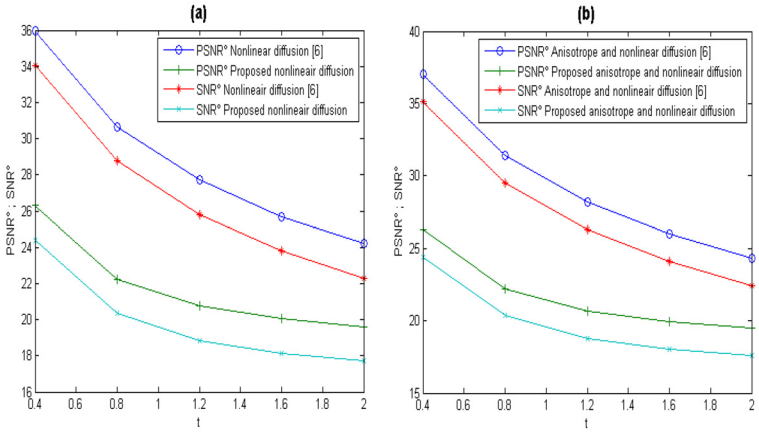

Figure 8. Comparison over the same image processing time interval, of the SNR^o and $PSNR^o$ values of our models with those of the models proposed by [6]. (a) Comparison of the values of SNR^o and $PSNR^o$ of the generalized nonlinear diffusion model $(a = 1;\ n = 3;\ \rho = 0.1;\ dt = 0.01)$ with those of the nonlinear diffusion model $(\alpha = 0.5; \beta = 1; dt = 0.01)$ proposed [6]. (b) Comparison of the values of SNR^o and $PSNR^o$ of the generalized anisotropic and nonlinear diffusion model $(a = 1;\ n = 3;\ \rho = 0.1;\ dt = 0.01;\ k = 0.03783)$ with those of the diffusion model anisotropic and nonlinear $(\alpha = 0.5;\ \beta = 1;\ dt = 0.01;\ k = 0.03783)$ proposed [6].

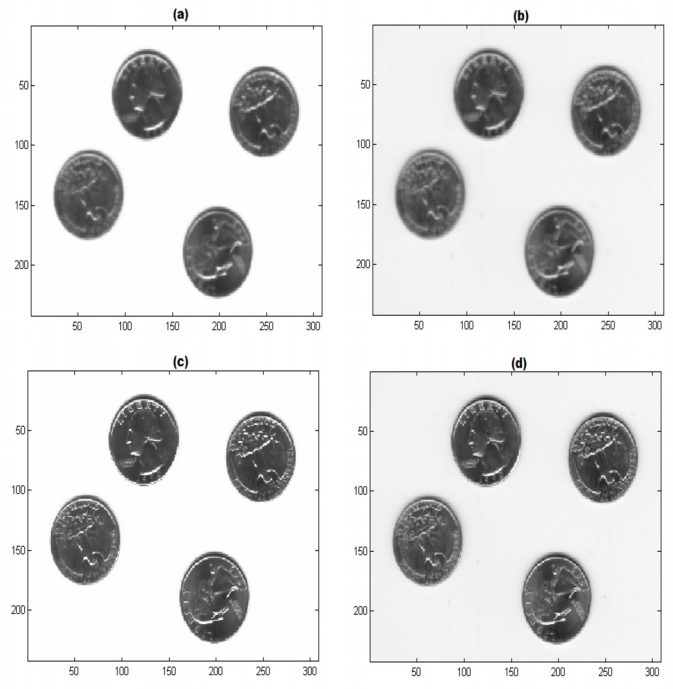

Figure 9. For the same restoration times $(t = 2)$, we compare the images restored by our models to the images restored by the models of [6]. (a) and (c) are the images restored respectively by the generalized model of nonlinear diffusion $(a = 1;\ n = 3;\ \rho = 0.1;\ dt = 0.01)$ and the generalized model of anisotropic and nonlinear diffusion $(a = 1;\ n = 3;\ \rho = 0.1;\ dt = 0.01;\ k = 0.03783)$, proposed in this study. (b) and (d) are the images restored respectively by the nonlinear diffusion model $(\alpha = 0.5;\ \beta = 1;\ dt = 0.01)$ and the anisotropic and nonlinear diffusion model $(\alpha = 0.5;\ \beta = 1;\ dt = 0.01;\ k = 0.03783)$, proposed by [6].

3.2. Sensitivity of image processing to model parameters

We analyzed the sensitivity of image processing to parameters n and a of the generalized nonlinear anisotropic diffusion model, using the $PSNR^o$ values as an assessment criterion.

First, we varied the values of the parameter n and fixed the values of the

other parameters at: $a = 1$, $\rho = 0.1$; $dt = 0.01$; $k = 0.03783$. Figure 10 (a) shows the variation of $PSNR^o$ as a function of time, for different values of the parameter n. We note, at $t = 2$, that the image is better restored with the lowest value of n, as confirmed in Figure 10 (b) where we observe an image which is partially restored for $n = 20$.

(a) (b)

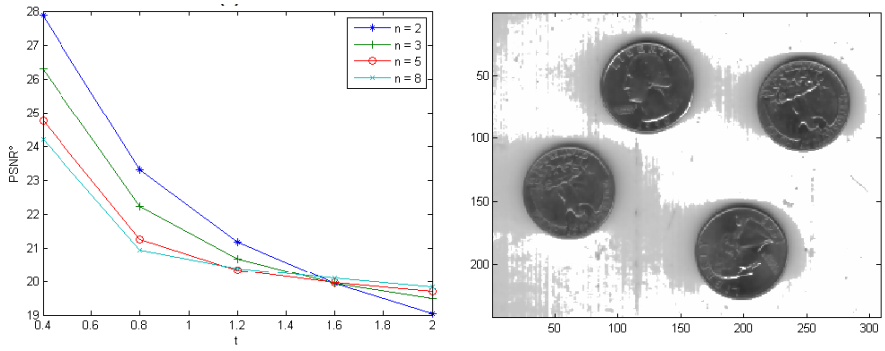

Figure 10. Here we describe the sensitivity of the image processing to the parameter n, with the generalized anisotropic and non-linear diffusion model, for the values of the parameters of the model: $a = 1$; $\rho = 0.1$; $dt = 0.01$; $k = 0.03783$. (a) shows the variation of $PSNR^o$ as a function of time, for different values of the parameter n, and (b) shows a partially restored image, with $n = 20$; $t = 2$.

Second, we varied the values of the parameter a and fixed the values of the other parameters at: $n = 3$; $\rho = 0.1$; $dt = 0.01$; $k = 0.03783$. Figure 11 (a) shows the variation of $PSNR^o$ as a function of time, for different values of the parameter a. We note, at $t = 2$, that the image is better restored with the highest value of a. For the same processing time, the same parameters and when $a = 10$; $\rho = 1.5$, we see that the model makes it possible to segment the images, as illustrated in Figures 11 (b) and 12.

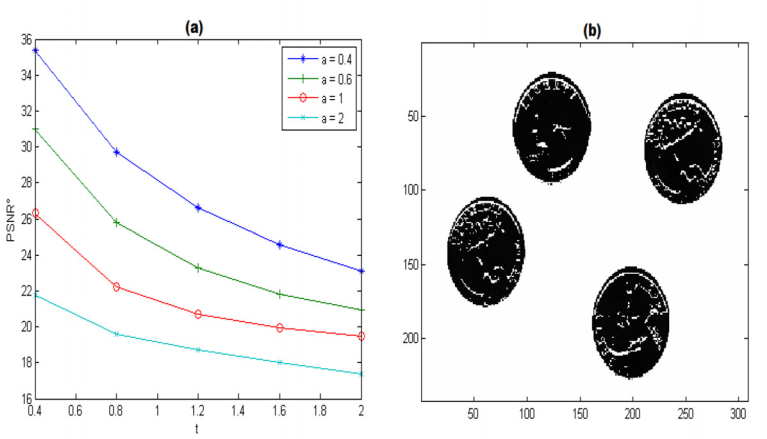

Figure 11. Here we describe the sensitivity of the image processing to parameter a, with the generalized anisotropic and nonlinear diffusion model, for the values of the parameters of the model: $n = 3$; $\rho = 0.1$; $dt = 0.01$; $k = 0.03783$. (a) shows the variation of $PSNR^o$ as a function of time, for different values of the parameter a; (b) shows the segmented image of the image studied, with $a = 10$; $\rho = 1.5$; $t = 2$.

Figure 12. (a) and (b) are the original images; (c) and (d) are their images segmented by the generalized nonlinear anisotropic diffusion model, with the values of the parameters of the model: $a = 10$; $n = 3$; $\rho = 1.5$; $t = 2$; $dt = 0.01$; $k = 0.03783$.

4. Conclusion

The application of the generalized anisotropic and nonlinear diffusion equation to image processing was the subject of this work. We have rewritten, in dimension 2, the generalized model of nonlinear diffusion in dimension 1 proposed by [43]. We then combined this model with the anisotropic diffusion model of [29] to obtain a generalized nonlinear anisotropic diffusion model. We used the digital resolution of these models to restore an image. The results show that the contrast of the degraded image is significantly improved and that the image is well restored. We assessed the quality of the restored images using a few statistical criteria. We also compared the quality of the images restored by our models to that of the

images restored by [6]. This comparison shows, over the same processing time, that the quality of the images restored by our models is better than that of the images restored by the models proposed by [6]. We also studied the sensitivity of the treatment to some parameters of our models. It turns out that for certain choices of parameters, one of our models is used to perform the segmentation of the images.

References

[1] S. Mitra and G. Sicuranza, Nonlinear image processing, Academic Press Series in Communications, Networking and Multimedia, 2001.

[2] J. F. Aujol, Contribution to the analysis of textures in image processing by variational methods and partial differential equations, Doctoral thesis, Universit Nice Sophia Antipolis, 2004.

[3] R. Deriche and O. Faugeras, Partial differential equations in image processing and computer vision, Journal Signal Processing 13(6) (1996), 551-577.

[4] V. M. Serge Soumanou, Siaka Massou and Sounmala Moumouni, Application of the one-dimensional reaction-diffusion equation solution to image restoration, Far East J. Appl. Math. 103(1) (2019), 13-27. DOI:10.17654/AM103010013

[5] T. Barbu and V. Barbu, A PDE approach to image restoration problem with observation on a meager domain, Nonlinear Analysis: Real World Applications 13(3) (2012), 1206-1215.

[6] S. Morfu, On some applications of diffusion processes for image processing, Physics Letters A 373 (2009), 2438-2444.

[7] Y. Shih, C. Rei and H. Wang, A novel PDE based image restoration: convection-diffusion equation for image denoising, Journal of Computational and Applied Mathematics 231(2) (2009), 771-779.

[8] T. Barbu, V. Barbu, V. Biga and D. Coca, A PDE variational approach to image denoising and restoration, Nonlinear Analysis: Real World Applications 10(3) (2009), 1351-1361.

[9] E. Bratsolis and M. Sigelle, Fast SAR image restoration, segmentation, and detection of high-reflectance regions, IEEE Trans. Geosci. Remote Sens. 41 (2003), 2890-2899.

[10] Y. You and M. Kaveh, Fourth-order partial differential equations for noise removal, IEEE Transactions on Image Processing 9 (2000), 1723-1730.

[11] L. Alvarez and L. Mazorra, Signal and image restoration using shock filters and anisotropic diffusion, SIAM Journal on Numerical Analysis 31 (1994), 590-605.

[12] L. Alvarez, F. Guichard, P. L. Lions and J. M. Morel, Axioms and fundamental equations of image processing, Archive for Rational Mechanics and Analysis 123 (1993), 199-257.

[13] T. Brox, M. Rousson, R. Deriche and J. Weickert, Colour, texture, and motion in level set based segmentation and tracking, Image and Vision Computing 28(3) (2010), 376-390.

[14] G. Chung and L. A. Vese, Image segmentation using a multilayer level-set approach, Computing and Visualization in Science 12(6) (2009), 267-285.

[15] L. He, Z. Peng, B. Everding, X. Wang, C. Y. Han, K. L. Weiss and W. G. Wee, A comparative study of deformable contour methods on medical image segmentation, Image and Vision Computing 26(2) (2008), 141-163.

[16] G. Chung and L. A. Vese, Energy minimization based segmentation and denoising using a multilayer level set approach, Energy Minimization Methods in Computer Vision and Pattern Recognition, Springer, Berlin, Heidelberg, 2005, pp. 439-455.

[17] M. Ebihara, H. Mahara, T. Sakurai, A. Nomura and H. Miike, Image Processing by a Discrete Reaction-Diffusion System, Proceedings Visualization, Imaging and Image Processing (VIIP 2003), Benalmadena, Spain, 2003, pp. 8-10.

[18] T. F. Chan and L. Vese, Active contours without edges, IEEE Trans. Image Processing 10(2) (2001), 266-277.

[19] I. Cohen, 2D and 3D deformable models: application to the segmentation of medical images, Ph.D. thesis, University Paris IX-Dauphine, 1992.

[20] I. Cohen, On active contour models and balloons, CVGIP: Image Understanding, 53 (1991), 211-218.

[21] P. Perona and J. Malik, A network for multiscale image segmentation, Proc. IEEE Int. Symp. Circuit and Systems (ISCAS-88) (1988), pp. 2565-2568.

[22] M. Kass, A. Witkins and D. Terzopoulos, Snakes: active contour models, International Journal of Computer Vision 1(4) (1988), 321-331.

[23] Gerlind Plonka and Jianwei Ma, Nonlinear Regularized Reaction-Diffusion Filters for Denoising of Images with textures IEEE Transactions on Image Processing 17(8) (2008), 283-1294. DOI : 10.1109/TIP.2008.925305.

[24] Allen R. Sanderson, Robert M. Kirby, Chris R. Johnson and Lingfa Yang, Advanced Reaction-Diffusion Models for texture Synthesis, Journal of Graphics Tools 11(3) (2006), 47-71.

[25] Deborah R. Fowler, Hans Meinhardt and Przemyslaw Prusinkiewicz, Modeling seashells, Computer Graphics (SIGGRAPH), pp. 379-387, ACM Press, New York, NY, USA 1992.

[26] Greg Turk, Generating textures on arbitrary surfaces using reaction-diffusion, Computer Graphics (SIGGRAPH), pp. 289-298, ACM Press, New York, NY, USA, 1991.

[27] Andrew Witkin and Michael Kass, Reaction-diffusion textures, Computer Graphics (SIGGRAPH), pp 299-308, ACM Press, New York, NY, USA, 1991.

[28] A. M. Turing, The chemical basis of morphogenesis, Phil. Trans. Roy. Soc. Lond. B 237 (1952), 3772.

[29] P. Perona and J. Malik, Scale space and edge detection using anisotropic diffusion, IEEE Transactions on Pattern Analysis and Machine Intelligence 12(7) (1990), 629-239.

[30] Shin-Min Chao and Du-Ming Tsai, Astronomical image restoration using an improved anisotropic diffusion. doi:10.1016/j.patrec.2005.08.021.

[31] G. Gilboa, N. Sochen, Y. Zeevi, Forward-and-backward diffusion processes for adaptive image enhancement and denoising, IEEE Transactions on Image Processing 11(7) (2002), 689-703.

[32] G. Gilboa, Y. Zeevi and N. Sochen, Signal and image enhancement by a generalized forward-and-backward adaptive diffusion process, Proceedings of the X European Signal Processing Conference, EUSIPCO 2000, Tampere, Finland, 2000.

[33] F. Catte, P. L. Lions, J. M. Morel and T. Coll, Image selective smoothing and edge detection by nonlinear, SIAM Journal on Numerical Analysis 29(1) (1992), 182-193.

[34] J. Monteil and A. Beghdadi, A new adaptive nonlinear anisotropic diffusion for noise smoothing, Proceedings of the International Conference in Image Processing ICIP 98, Chicago, Illinois 3 (1998), 254-258.

[35] J. Weickert, Anisotropic Diffusion Filter for Image Processing: Based Quality Control, A. Fasano, M. Primicerio (Eds.), Proc. Seventh European Conf. on Mathematics in Industry, Teubner, Stuttgart, 1994, pp. 355-362.

[36] M. Ait Oussous, N. Alaa and Y. Ait Khouya, Anisotropic and nonlinear diffusion applied to image enhancement and edge detection, Int. J. Computer Applications in Technology 49(2) (2014).

[37] M. Black, G. Sapiro, D. Marimont and D. Heeger, Robust anisotropic diffusion, IEEE Transactions on Image Processing 7(3) (1998), 421-432. DOI: 10.1109/83.661192.

[38] J. D. Murray, Mathematical Biology: II, Spatial Models and Biomedical Applications, 3rd ed., Springer, New York, 2003.

[39] S. Morfu, B. Nofiele and P. Marquie, Phys. Lett. A 367 (2007), 192-198.

[40] S. Morfu, P. Marquie, B. Nofiele and D. Ginhac, Advances in Imaging and Electron Physics, Elsevier 152 (2008), 79153.

[41] J. Nagumo, S. Arimoto and S. Yoshizawa, An active pulse transmission line simulating nerve axon, Proceedings of the I.R.E. 50(10) (1962), 2061-2070.

[42] R. Fitz Hugh, Impulses and physiological states in theoretical models of nerve membrane, Biophysical Journal 1(6) (1961), 445-466.

[43] S. Moumouni, V. M. S. Soumanou, S. Massou, A. L. Essoun and M. Tchoffo, Generalization and resolution of the homogeneous reaction-diffusion equation by the method of factorization of ordinary differential operators, Advances in Differential Equations and Control Processes 17(4) (2016), 265-283. DOI: 10.17654/DE017040265